Supporting Information

Roles of Ga^{3+} promoter for direct synthesis of iso-butanol via syngas over K-ZnO/ZnCr$_2$O$_4$ catalyst

Tao Zhang[a], Chunyang Zeng[b], Yingquan Wu[a], Nana Gong[a,c], Jiaqian Yang[a,c], Guohui Yang[a], Noritatsu Tsubaki[d*], Yisheng Tan[a*]

[a] State Key Laboratory of Coal Conversion, Institute of Coal Chemistry, Chinese Academy of Science, Taiyuan, Shanxi 030001, China

[b] China Petroleum Chemical Industry Federation, Beijing 100723, China

[c] University of Chinese Academy of Science, Beijing 100049,China

[d] Department of Applied Chemistry, School of Engineering, University of Toyama, Gofuku 3190,Toyama,930-8555, Japan

1. Computational methods

The periodic DFT calculation was performed by using Vienna ab initio simulation Package (VASP) [1-4]. The generalized gradient approximation with the Perdew-Burke-Ernzerh functional was used to deal with the electron exchange-correlation energy. The projector-augmented wave method was used to describe the interactions between electrons and atomic cores, the cutoff energy for the plane-wave basis set was 450 eV. Van der Waals interaction was taken into consideration by DFT-D3 method. The geometry optimizations was performed by conjugate gradient algorithm (IBRION=2) and quasi-Newton algorithm (IBRION=1) with the convergence criterion for energy and force were less than 10^{-5} eV and 0.02 eV/Å, respectively. A $1\times1\times1$ k-point grid method was applied to sample the Brillouin zone. The transition state seeking for the elementary reactions of CO activation was studied by climbing image nudged elastic band (CI-NEB) method[5]. The obtained saddle point was confirmed by frequency analysis to have a single imaginary

frequency. All the surface atoms were fixed except for the relaxation of the adsorbed molecule or groups such as CO, C, H, CHO during CI-NEB calculations based on our computational resources.

The adsorption energies of related adsorbed species such as CO, CHO, H_2O and CO_2 were computed by the formula: $E_{ads} = E_{x/slab} - (E_x + E_{slab})$, where $E_{x/slab}$, E_{slab} and E_x are the total energies of species absorbed on the slab, the slab and the isolated gas species, respectively. The reaction energy ΔE and activation energy E_a are evaluated through the following equation (2) and (3):

$$\Delta H = E_{fs} - E_{is} \qquad (2)$$

$$E_a = E_{ts} - E_{is} \qquad (3)$$

where E_{fs}, E_{is} and E_{ts} are the energies of products, reactants and transition state, respectively.

2. Models

2.1 The possible locations of Ga^{3+} in $ZnCr_2O_4$

The possible locations of Ga^{3+} in the doped K-ZnO/$ZnCr_2O_4$ catalyst were confirmed by DFT calculation. The flowing possible locations of Ga^{3+} were fall in our consideration, that is (1) Zn^{2+} located at ZnO was replaced by Ga^{3+}, demoted as $Zn_{1/2}Ga_{1/2}O$, (ZGO); (2) Zn^{2+} located at the tetrahedron site of $ZnCr_2O_4$ was replaced by Ga^{3+}, denoted as $ZnCr_{16/7}Ga_{1/7}O_{34/7}$, (ZG); (3) Cr^{3+} located at the octahedral site of $ZnCr_2O_4$ was replaced by Ga^{3+}, denoted as $ZnCr_{15/8}Ga_{1/8}O_4$, (CG); (4) Ga^{3+} located at the vacancies in the bulk of $ZnCr_2O_4$. In addition, the possibility of ZGO, ZG, CG, and $ZnGa_2O_4$ formation through ZnO, γ- Ga_2O_3 , Cr_2O_3 , and $ZnCr_2O_4$ were also calculated to explore the possible origins of $ZnGa_2O_4$, or Ga adopted ZnCr spinel. The detailed reactions that fall our consideration are listed in Table s1.

The binding energy E_B is calculated by the following expression to test the phase stability of Ga adopted ZnCr oxide: a larger E_B indicates that the structure is most likely to exist and be stable, that is :

$$E_B = \sum E_{atom} n_{atom} - E_t$$

where E_t is the total energy of the constructed crystal lattice, E_{atom} is the total energy of isolated atom (Zn, Cr, Ga, and O, respectively) in vacuum, n_{atom} is the number of the atom that composed the crystal[6, 7]. The formation energies were calculated based on the most stable oxides phases as references states according to David A. Andersson et al 's strategy [8].

2.2 Adsorption of Ga on(311), (310), and (202) surfaces of $ZnCr_2O_4$

The (311), (310) and (202) surfaces of $ZnCr_2O_4$ were obtained by cutting the respective surfaces of the optimized $ZnCr_2O_4$ spinel. Among all these surfaces, tri-coordinated oxygen atoms were chosen as the preferred adsorption sites, other coordination unsaturated atoms such as Zn and Cr on the surface are fall out of our investigation owing to the fact that the electronegativity of these two atoms are much smaller than atom O. K-point grid method for the three surfaces are $3\times4\times1$ for (311) surface, $3\times2\times1$ for (310) surface and $2\times2\times1$ for (202) surface respectively, which was applied to sample the Brillouin zone.

3. Location of Ga atom in $ZnCr_2O_4$ spinel

The possible locations of Ga atom in the doped $ZnCr_2O_4$ proposed above were verified by DFT calculation. When Ga located on the vacancies of $ZnCr_2O_4$ crystal were investigated, the disorder of the spinel was observed obviously, implying that Ga could not exist in the locations of vacancies of ZnCr spinel. So the possible location of ZG and CG are our main consideration. The obtained structures and energies of CG and ZG are listed in Fig.s1 and Table s1. It is obviously show that when the configuration Zn^{2+} located in tetrahedron site, a much lower energy was obtained (-438.527 eV vs.-334.680 eV), indicating that Ga^{3+} located in the tetrahedron site is the most possible configurations of Ga^{3+} doped ZnCr spinel.

Based on the above analysis, $ZnCr_2O_4$(111), ZG(111), and $ZnGa_2O_4$(111) surfaces were constructed to mimic the surface structure of ZnCr spinel, Ga adopted ZnCr spinel and ZnGa spinel catalysts to further study the absorption and activation of syngas. Configurations of the two model catalyst were listed in Fig. S2. The adsorption of CO, CHO and COH were evaluated with the optimized structure and

adsorption energies listed in Fig. S3. As can been see in Fig.S3, on both catalyst surface CO prefers to absorbed on Cr site with atom C, with the adsorption energy for on the two catalyst surface are 1.20 eV and 2.70 eV respectively, indicating the replacement of Zn^{2+} by Ga^{3+} is advantageous to CO adsorption. In addition, the analysis to the most stable configurations of CO show that when Zn was replaced by Ga, C=O bond was enlarged from 1.16 Å to 1.17 Å, the distance between C and surface Cr is shorted from 1.98 Å to 1.91 Å. The stretching vibration of C-O bond decreased from 2024 cm^{-1} in the gas phase to 1979.22 cm^{-1} on $ZnCr_2O_4$ (111) surface and 1903.68 cm^{-1} on Zn-Ga (111) surface, which further verify the enhanced adsorption of CO by Ga addition. Formyl group formation through CO hydrogenation was also investigated by CI-NEB analysis. The results show (Fig.S4) that with Ga addition, the reaction energy was reduced from 0.24 eV to -1.05 eV, the activation energy of the two reactions reduced from 0.96 eV to 0.78 eV, indicating CHO formation becomes more preferable with Ga addition.

ZnCr₂O₄

ZG

CG

ZnGa₂O₄

ZGO

● Cr ● Ga ● Zn ● O
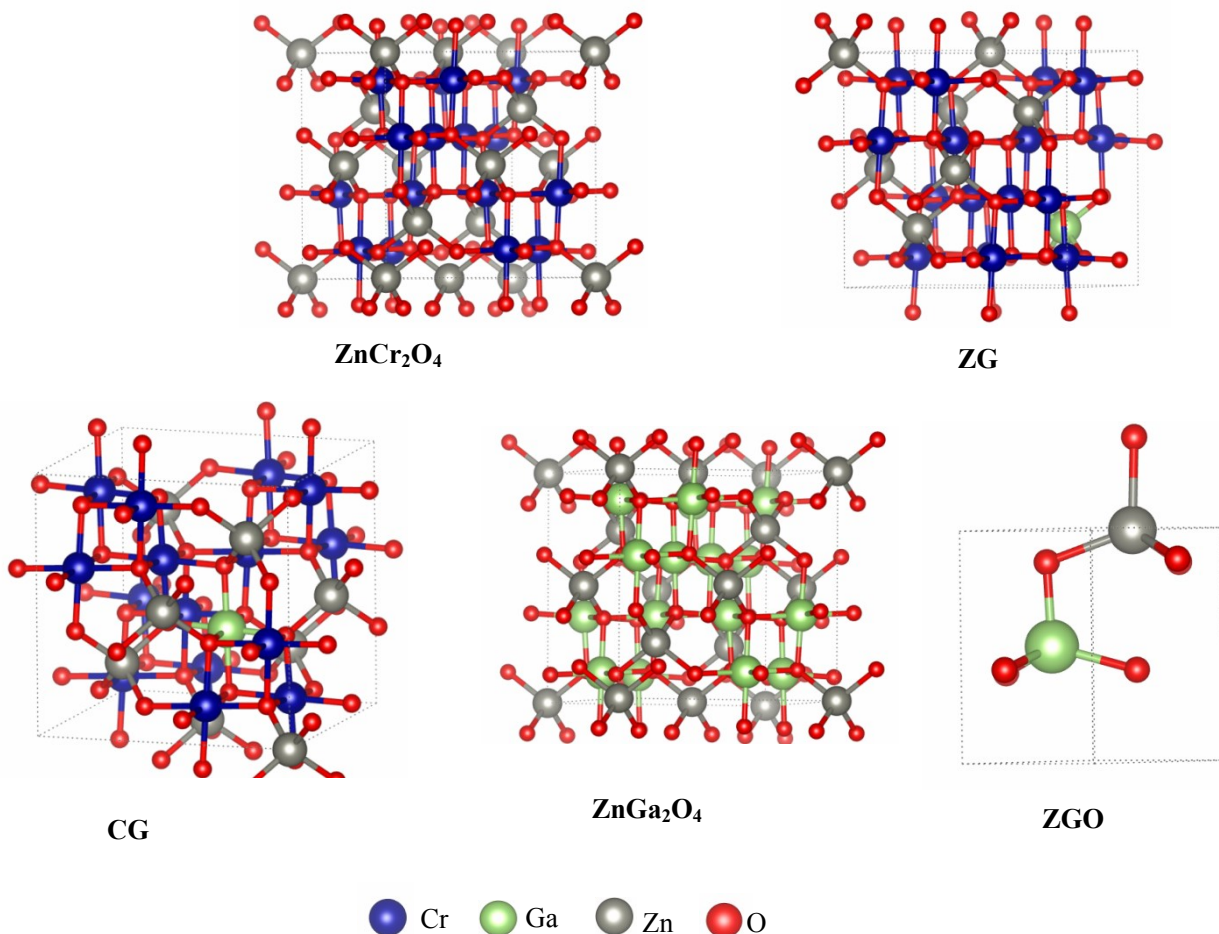
Schematic diagram of crystal structure for $ZnCr_2O_4$, ZG, CG, $ZnCa_2O_4$ and ZGO.
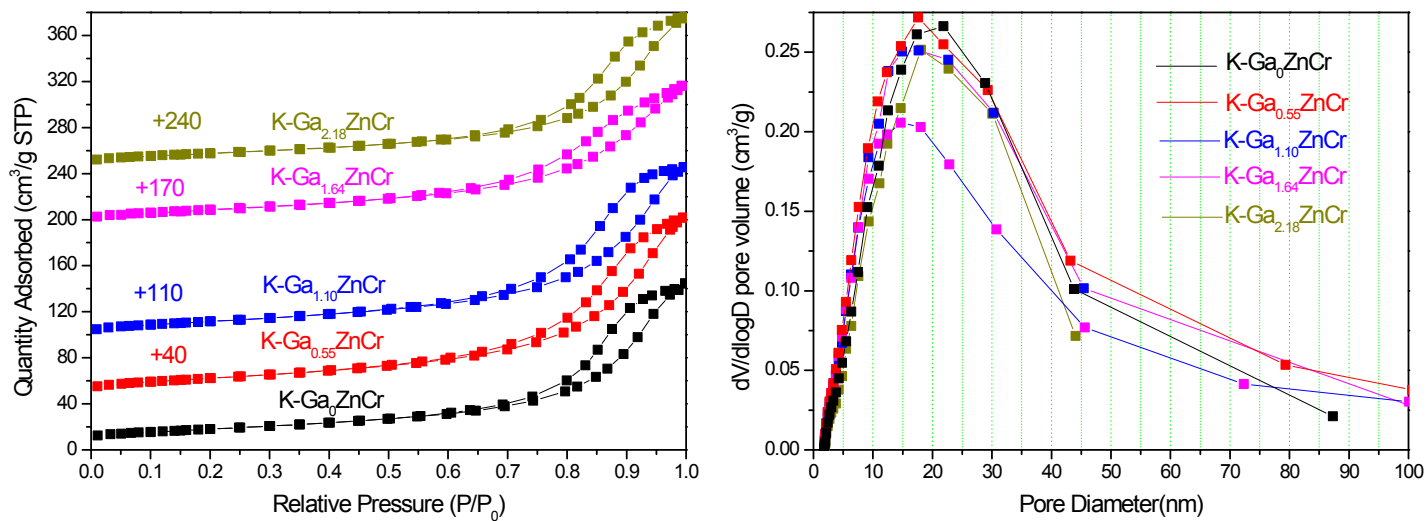
Fig. s1. Isotherm linear plot (left) and BJH desorption of dV/dD pore volume(right) for K-GaxZnCr samples. (x=0.0, 0.55, 1.10, 1.64 and 2.18)
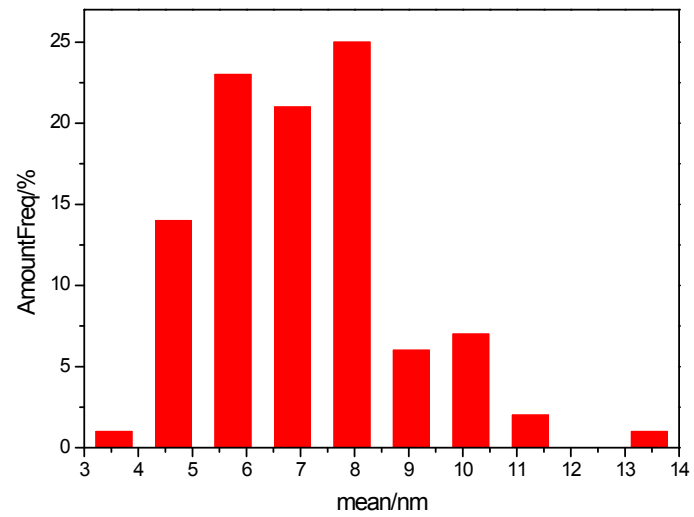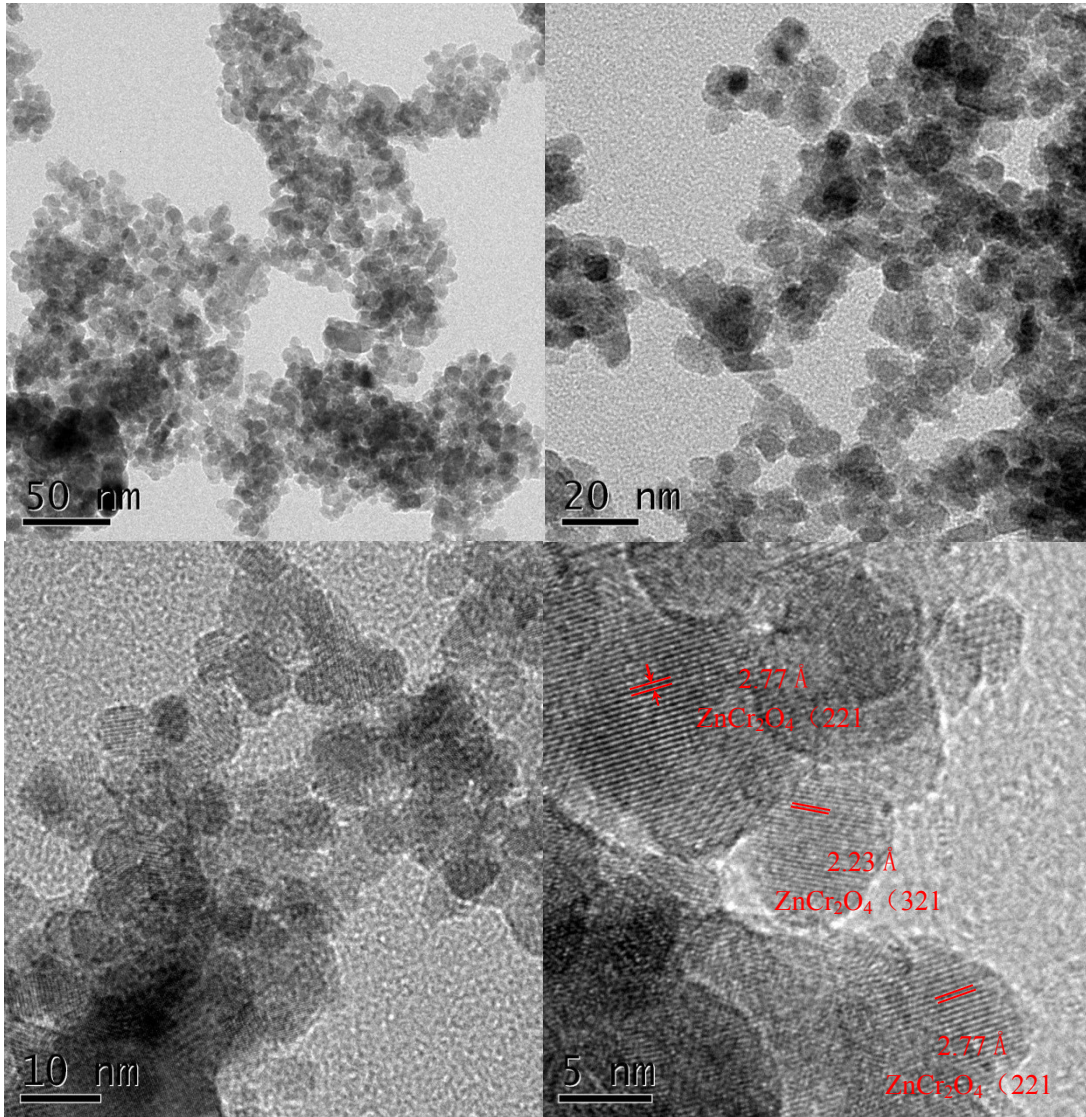
2.77 Å
ZnCr$_2$O$_4$（221

2.23 Å
ZnCr$_2$O$_4$（321
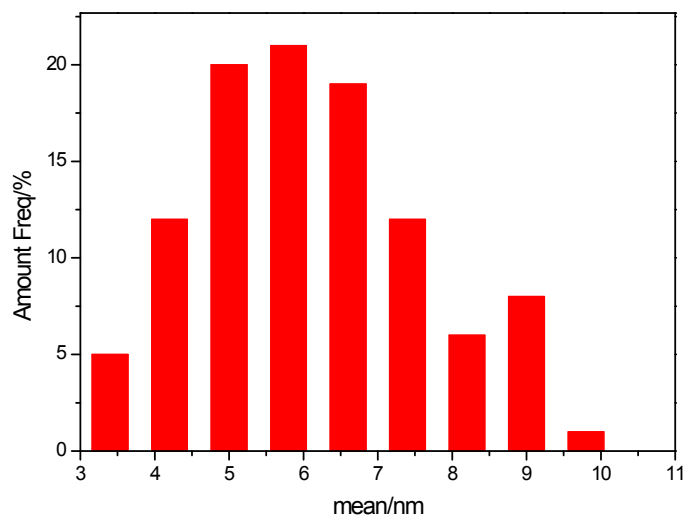
2.77 Å
ZnCr$_2$O$_4$（221
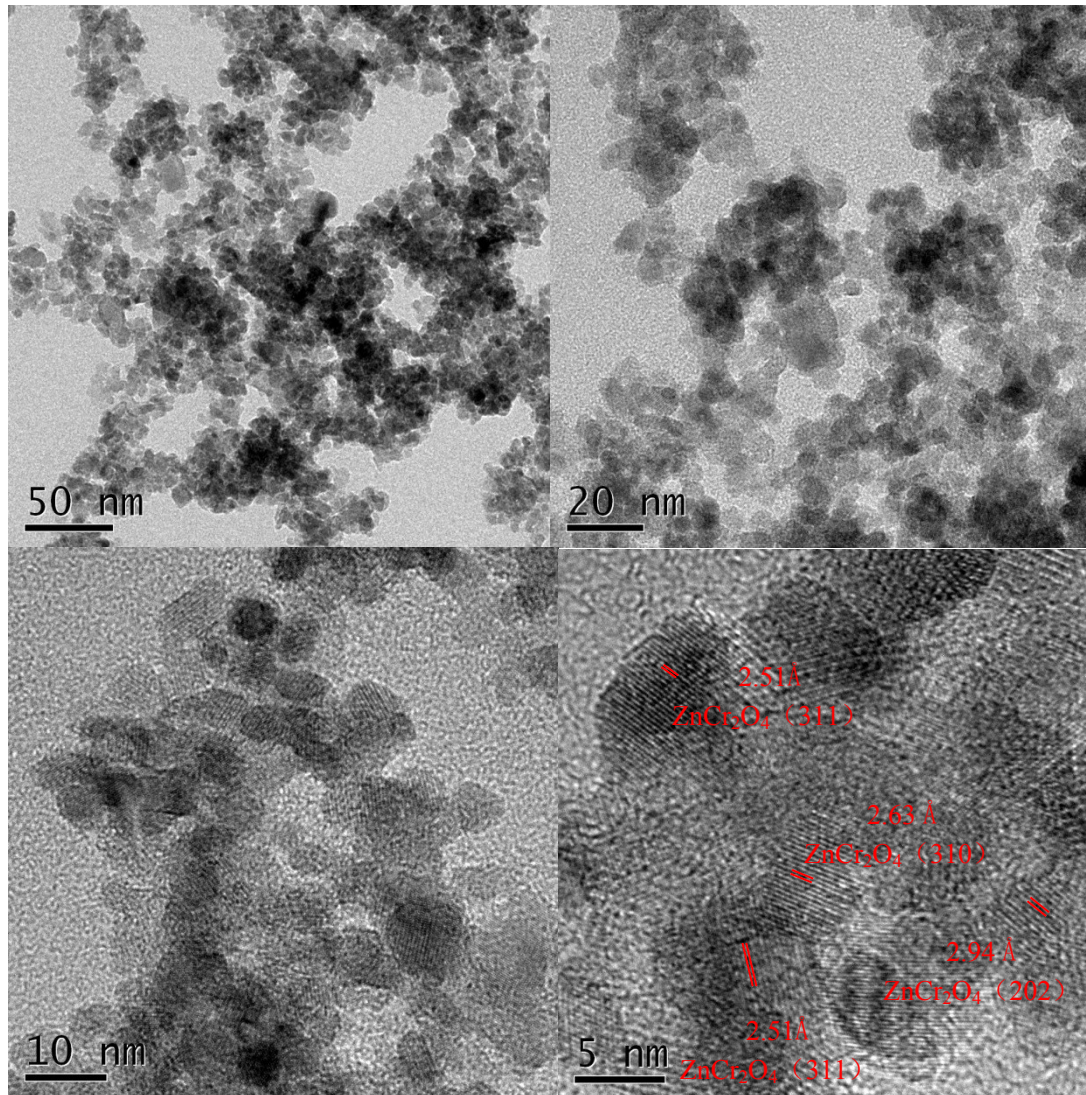
Fig.s2 HR-TEM images of K-Ga$_0$ZnCr catalyst.
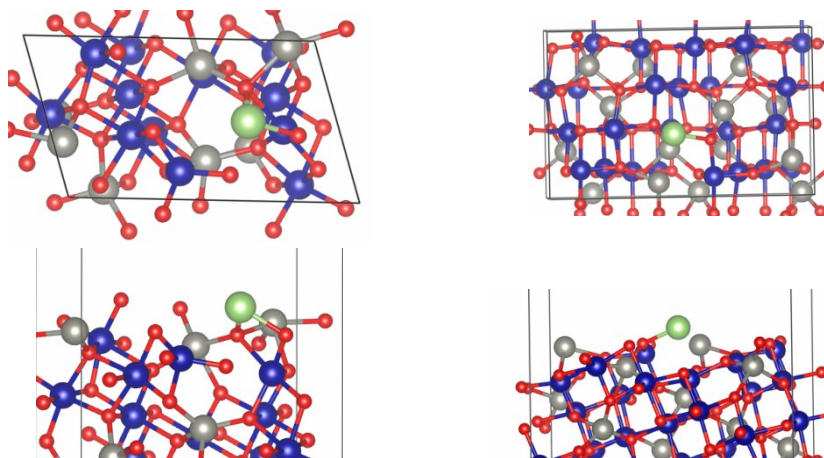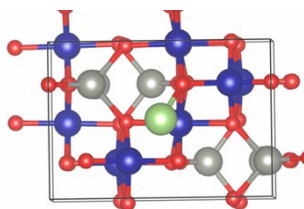
Fig.s3 HR-TEM images of K-Ga$_{1.10}$ZnCr catalyst.
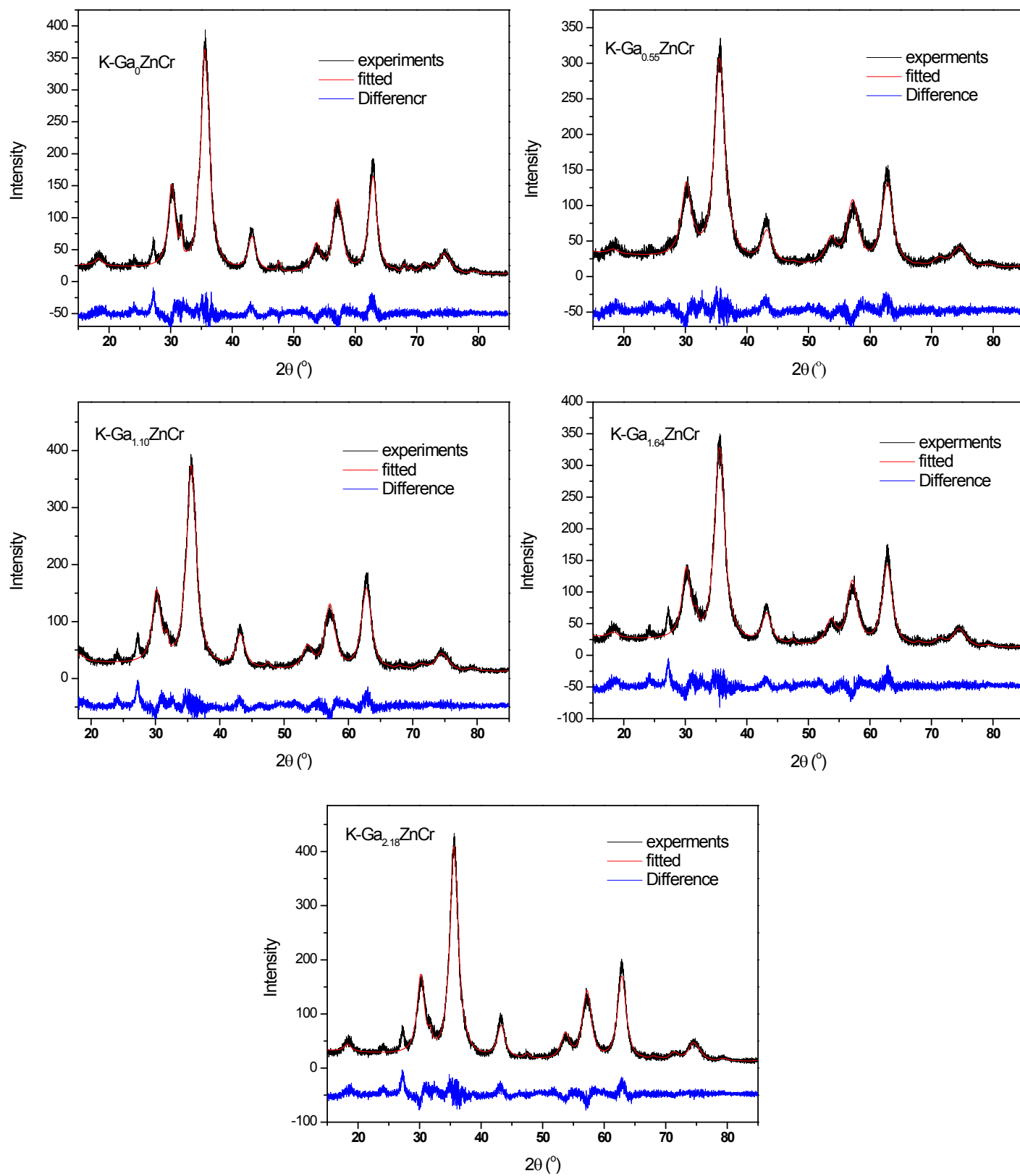
Fig. s4. Rietveld refinement results to the XRD patterns of K-Ga$_x$ZnCr catalysts.

Ga on (311) of ZnCr$_2$O$_4$

Ga on (310) of ZnCr$_2$O$_4$

Ga on (202) of ZnCr$_2$O$_4$

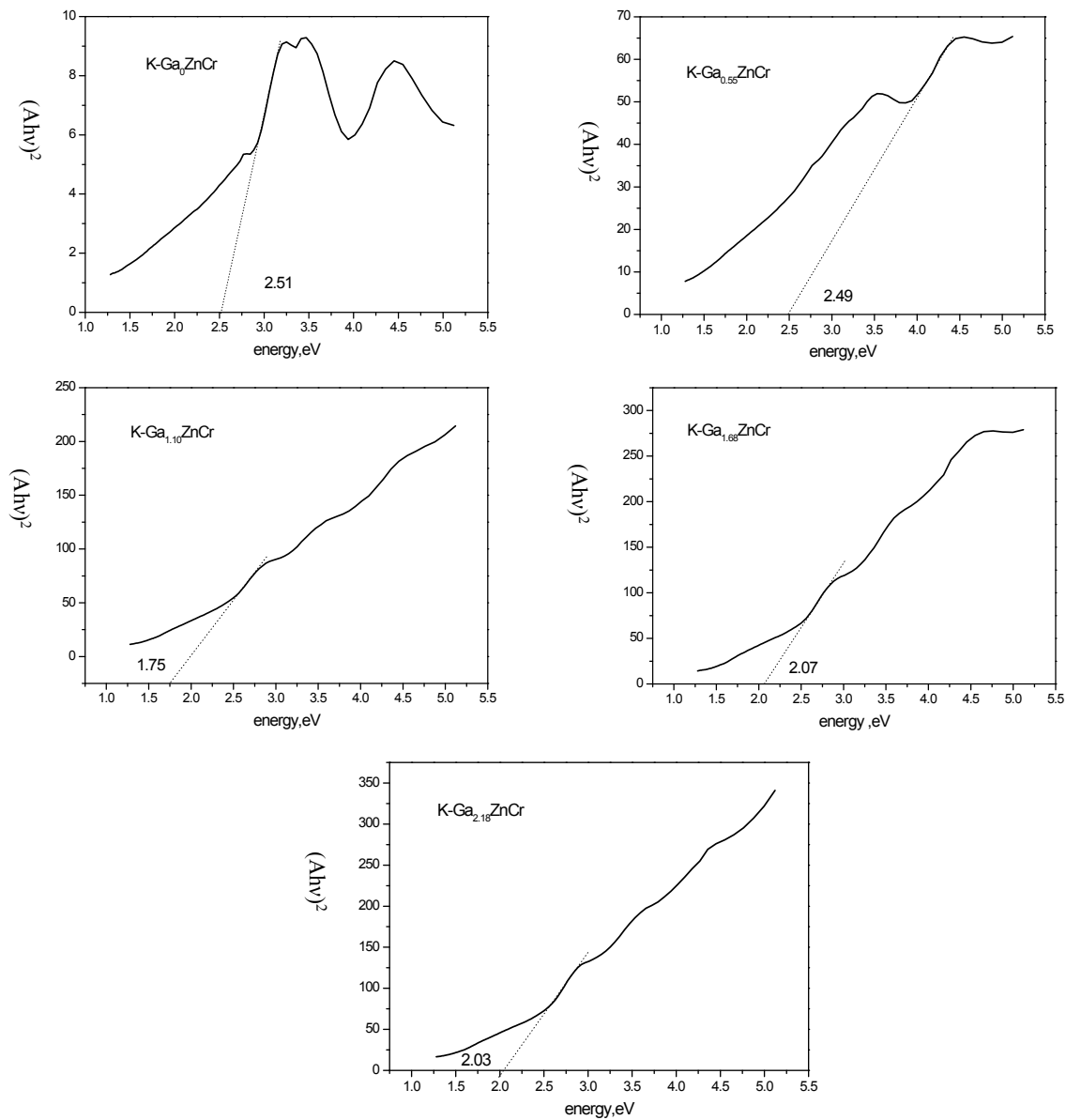**Fig.s5. Top view and side view of the configurations of Ga adsorbed on the (311), (310) and (202) surfaces of ZnCr$_2$O$_4$.**

Fig. s6. Indirect band gap E_g calculated from ultraviolet-visible diffuse reflectance spectral for K-Ga$_x$ZnCr catalysts.
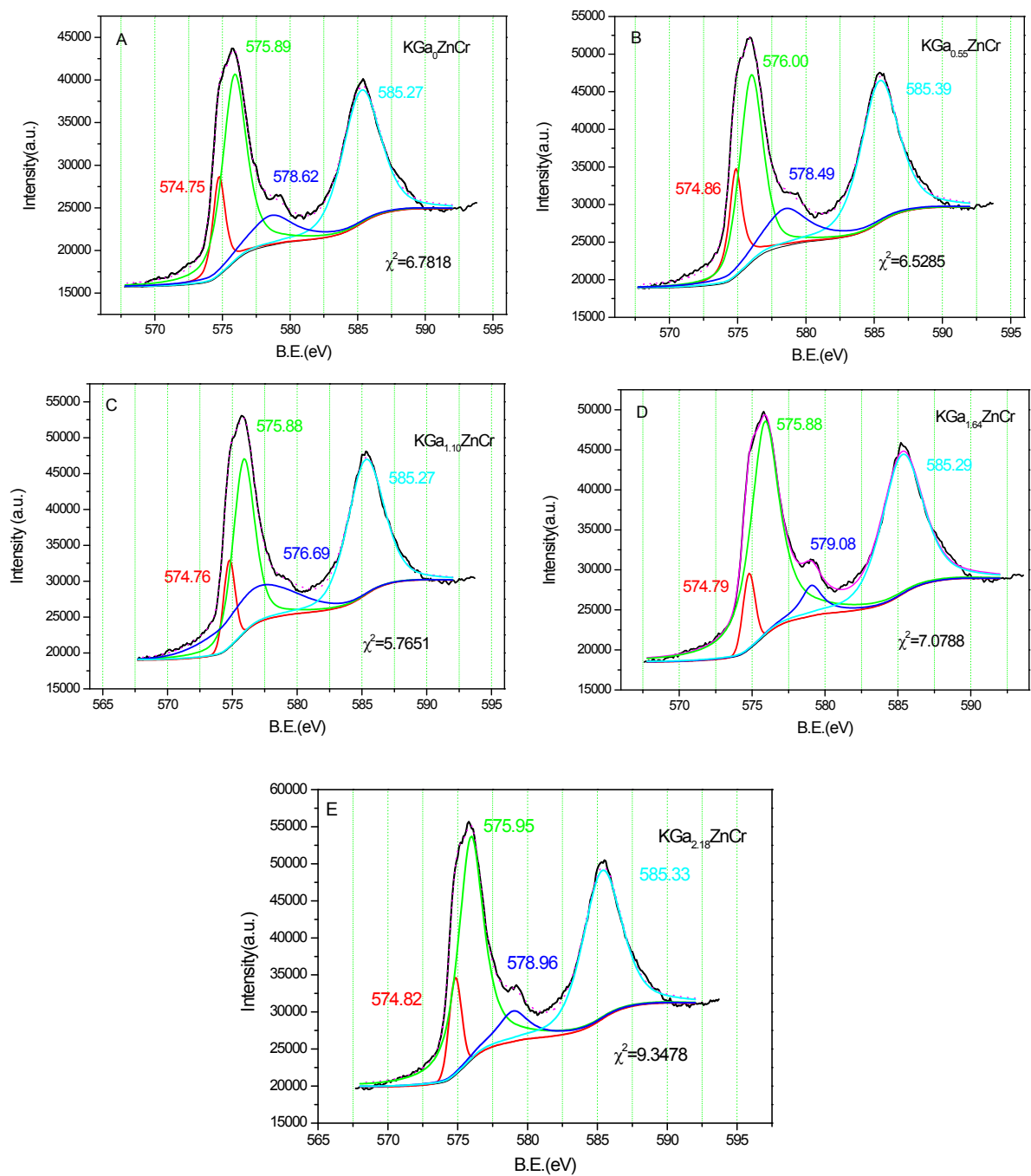
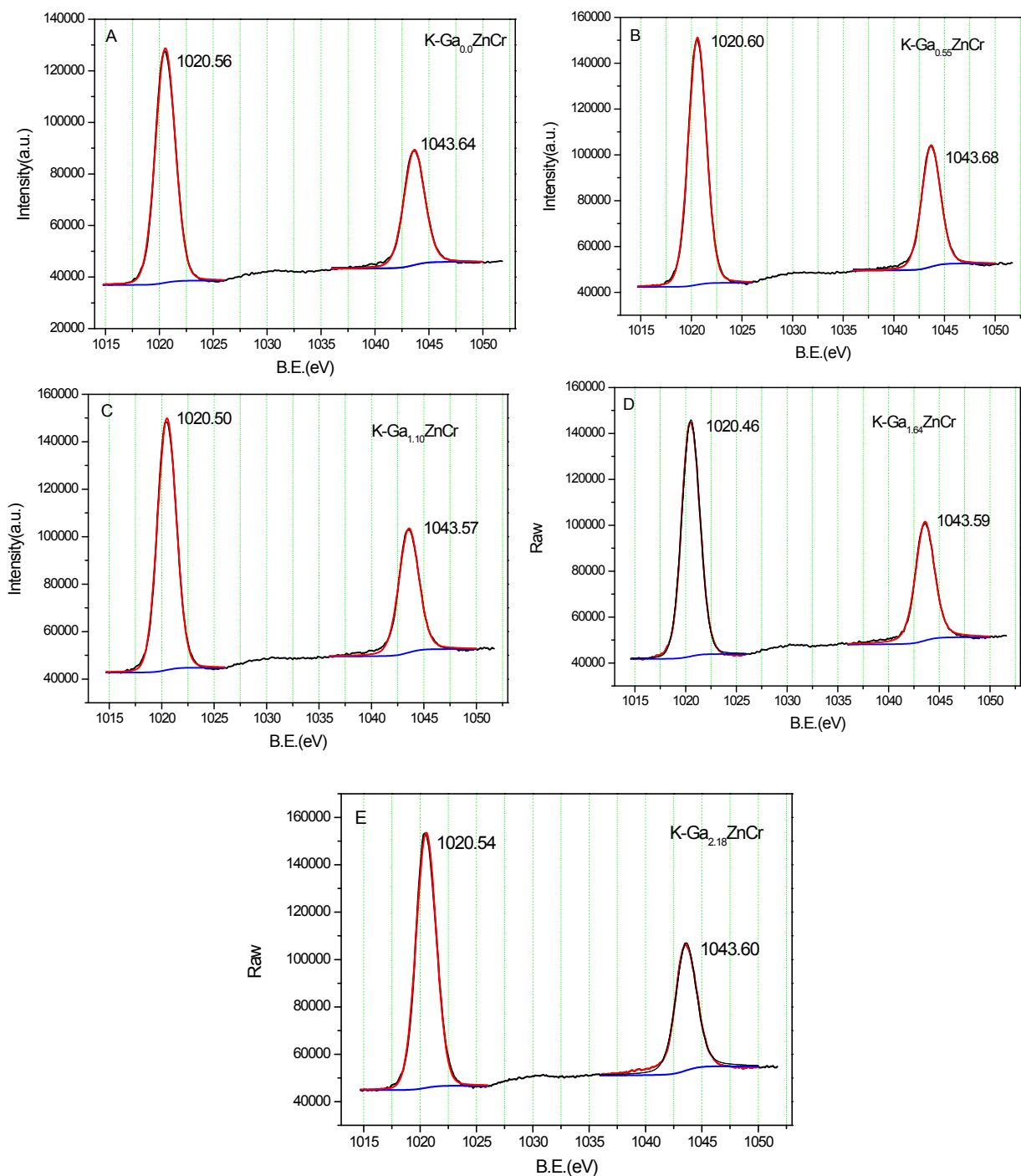**Fig. s7. The XPS spectral of Cr$_{2p}$ for K-Ga$_x$ZnCr samples. (x=0.0, 0.55, 1.10, 1.64 and 2.18)**

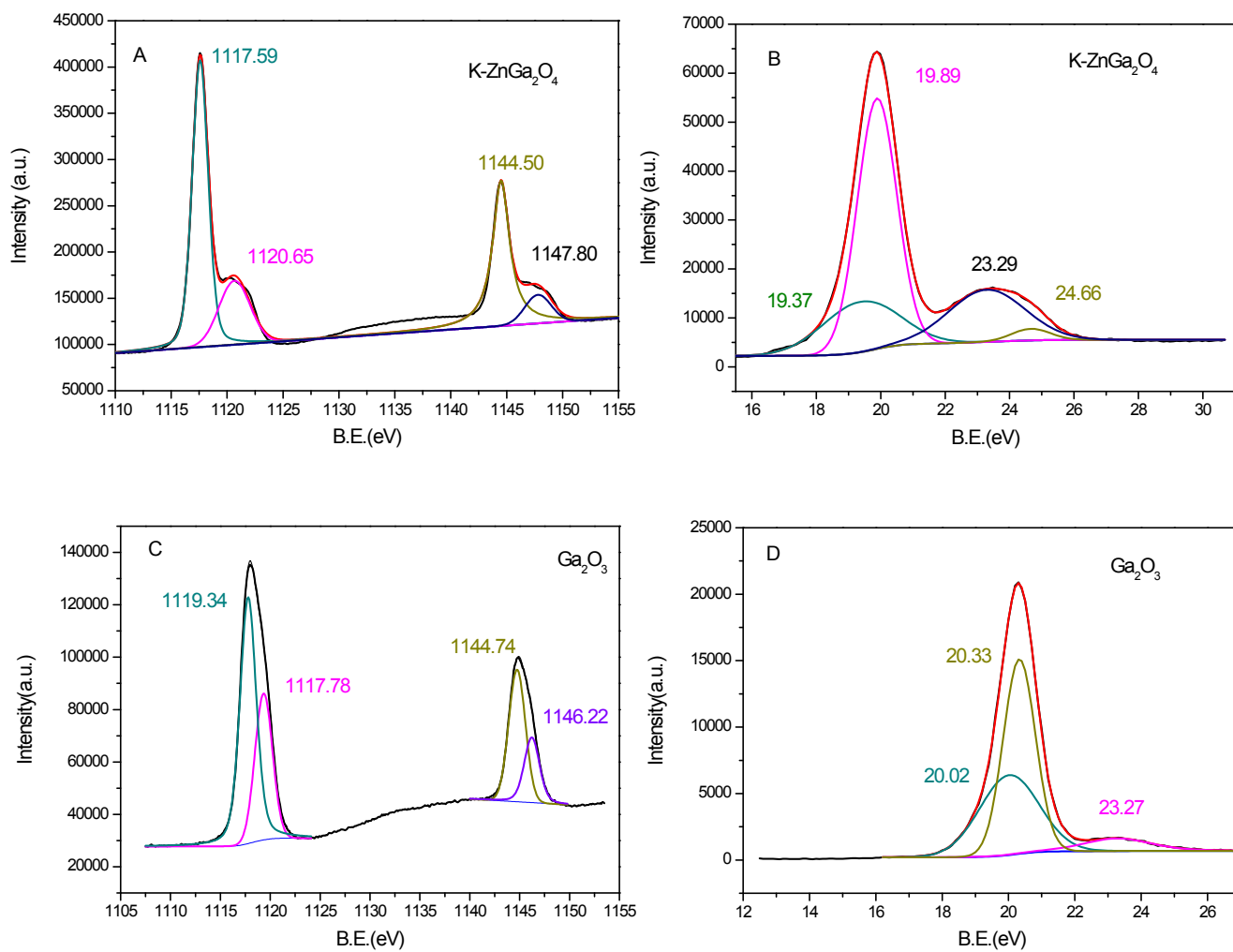**Fig. s8. The XPS spectral of Zn_{2P} for K-Ga_xZnCr samples. (x=0.0, 0.55, 1.10, 1.64 and 2.18)**

Fig. s9. The XPS spectrals of Ga2p for K-ZnGa$_2$O$_4$(A), Ga$_2$O$_3$(C) and Ga3d for K-ZnGa$_2$O$_4$ (B), Ga$_2$O$_3$ (D).

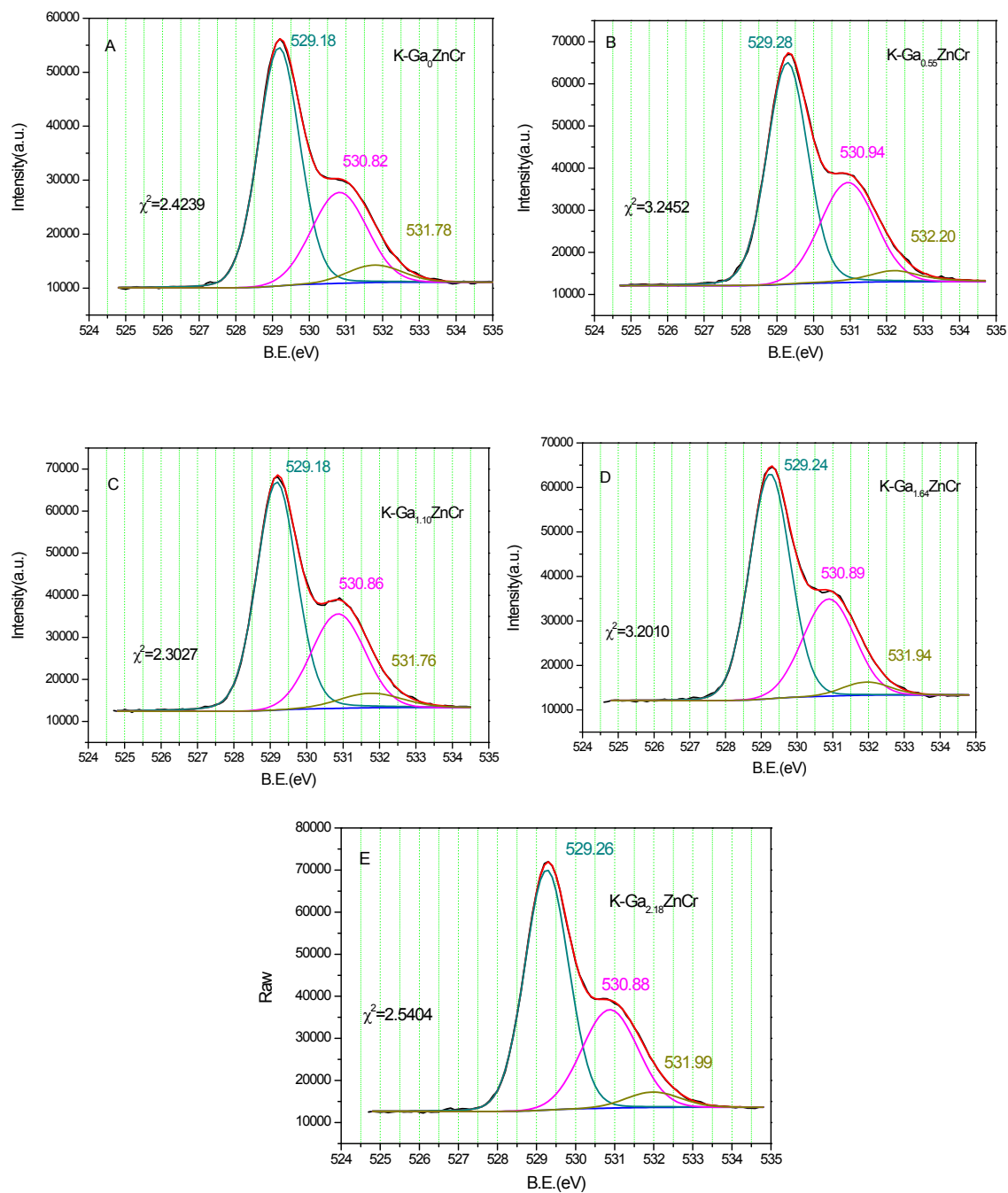Ga$_2$O$_3$ (99.99%) was perched from Shanghai Aladdin Biochemicl Technology Co.Ltd

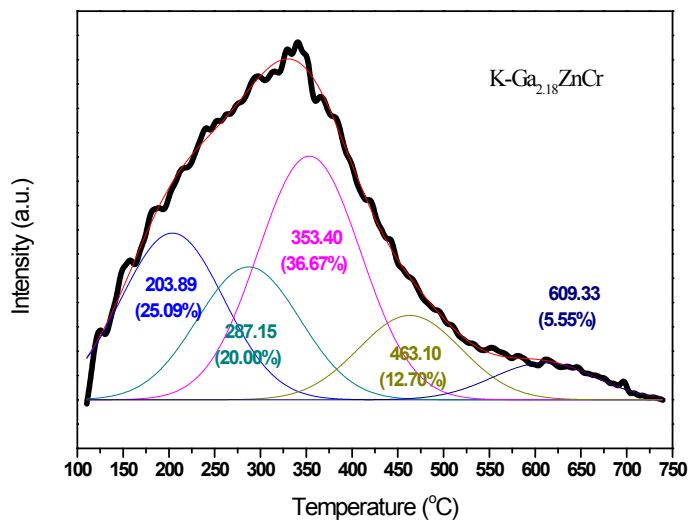**Fig. s10. The XPS spectral of O1s for K-Ga$_x$ZnCr samples. (x=0.0, 0.55, 1.10, 1.64 and 2.18)**
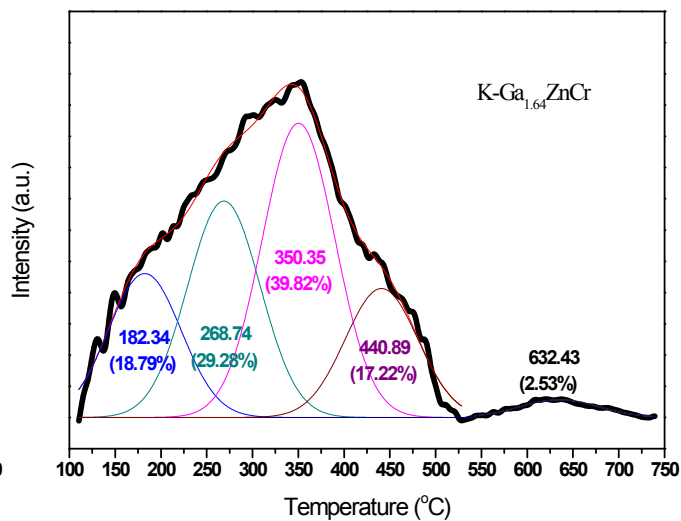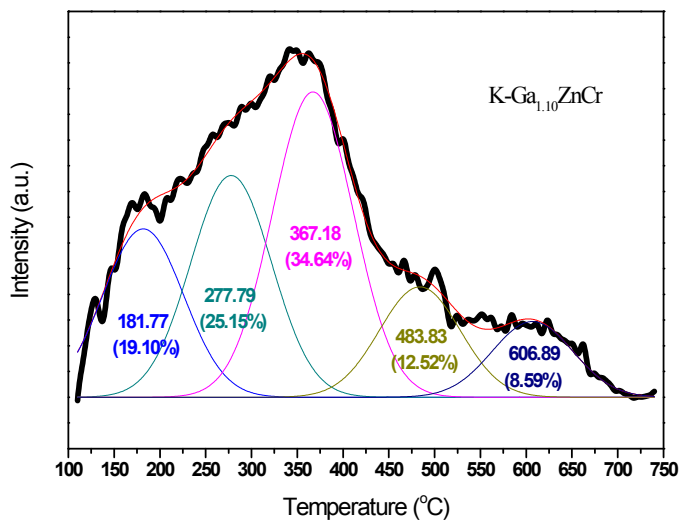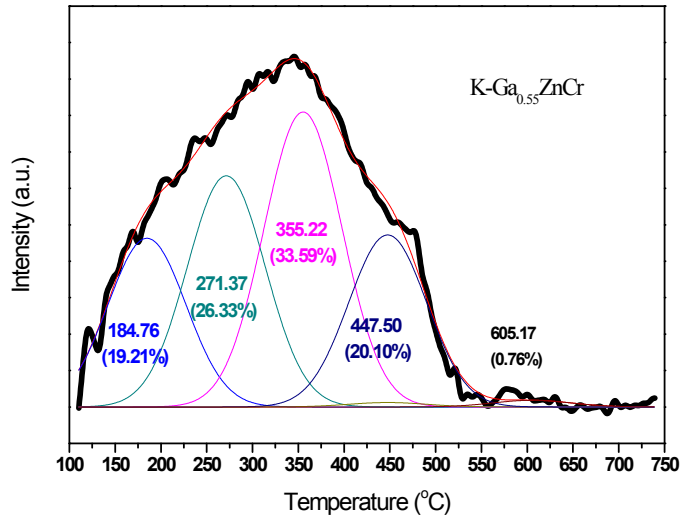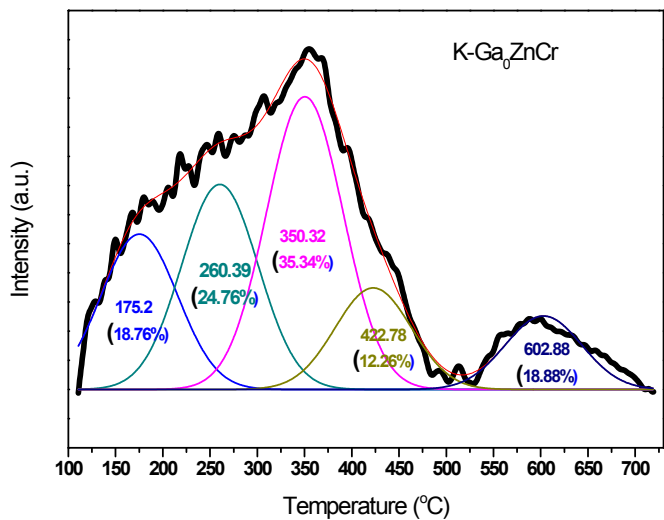
Fig. s11. TheCO$_2$-TPR profiles for K-Ga$_x$ZnCr samples. (x=0.0, 0.55, 1.10, 1.64 and 2.18)
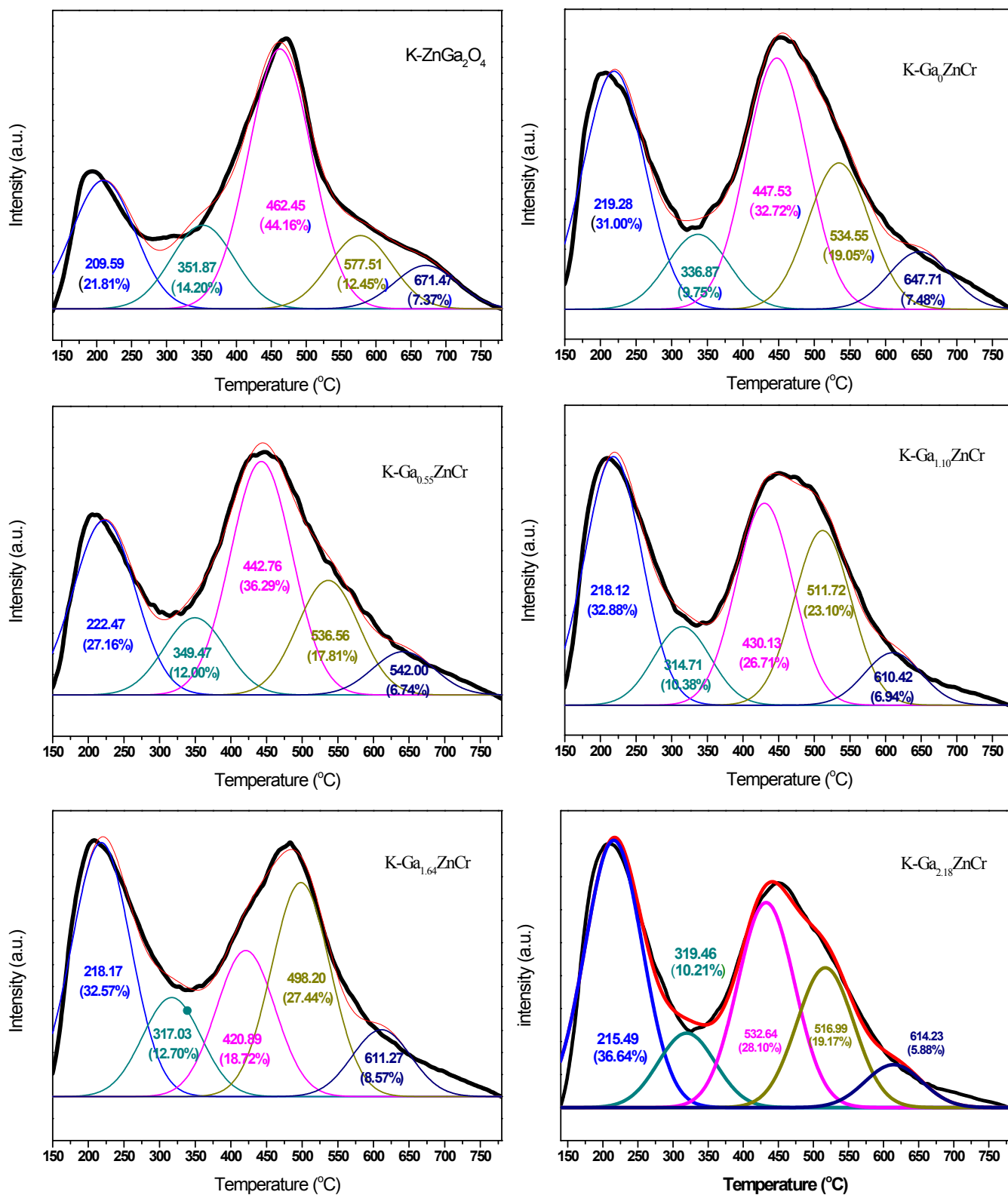
Fig. s12. The NH3-TPR profiles for K-ZnGa$_2$O$_4$ and K-Ga$_x$ZnCr samples. (x=0.0, 0.55, 1.10, 1.64 and 2.18)

Cr Ga Zn O H
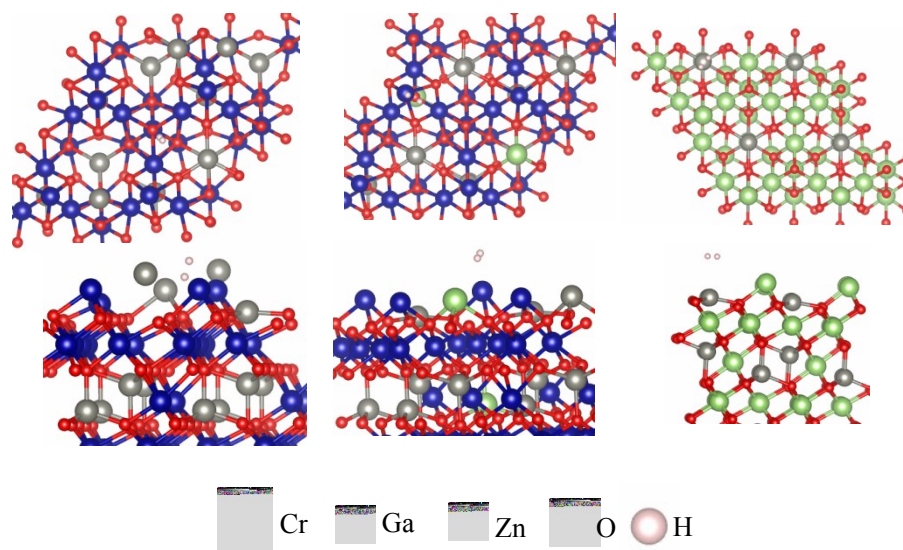
Fig. s14. The most stable adsorption configurations of H$_2$ on ZnCr$_2$O$_4$ (111) surface, ZG(111) surface, and ZnGa$_2$O$_4$ (111) surface.

surface	E$_{ads}$, eV	d$_{H-Me}$	d$_{H-H}$	frequency，cm^{-1} v_{H-H}, δ_{H-H}
ZG (111)				
ZnCr$_2$O$_4$ (111)	-2.84	1.98, 1.95	0.79	3647.45， 1153.53
ZnGa$_2$O$_4$ (111)	-1.01	2.57, 2.57	0.76	4122.89
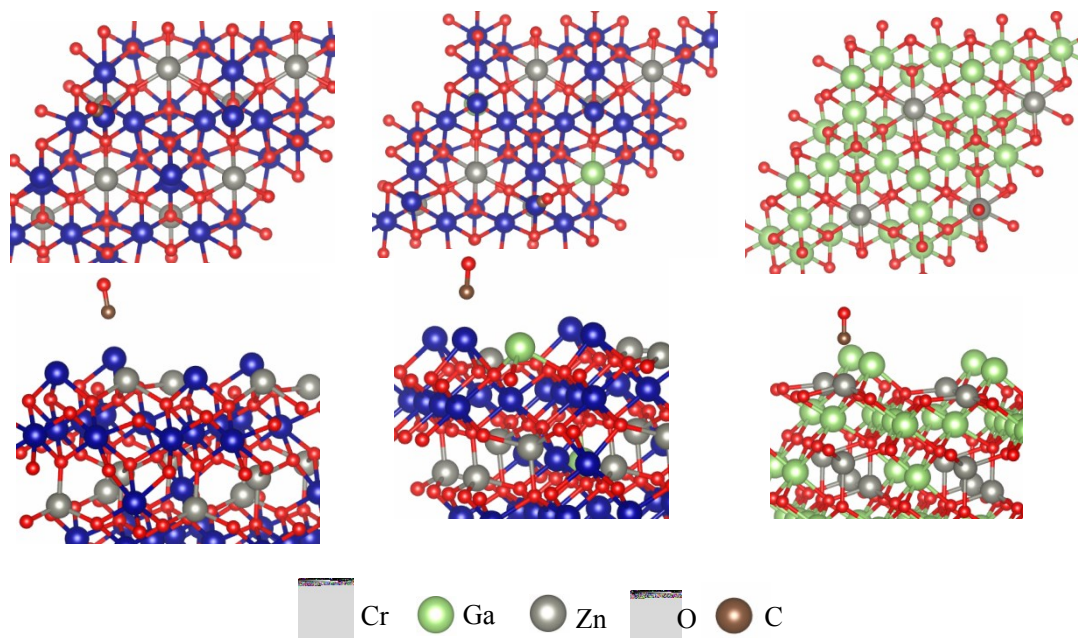
Fig. s15. The most stable adsorption configurations of CO on ZnCr₂O₄ (111) surface, ZG(111) surface, and ZnGa₂O₄ (111) surface.

surface	E_{ads}, eV	d_{C-Me}	d_{O-C}	frequency, cm^{-1} v_{CO}
ZG (111)		1.958	1.169	1931.64
ZnCr₂O₄ (111)	-0.71	1.978	1.161	1979.21
ZnGa₂O₄ (111)	-0.36	2.133	1.142	2110.31
CO			1.13	2124.27
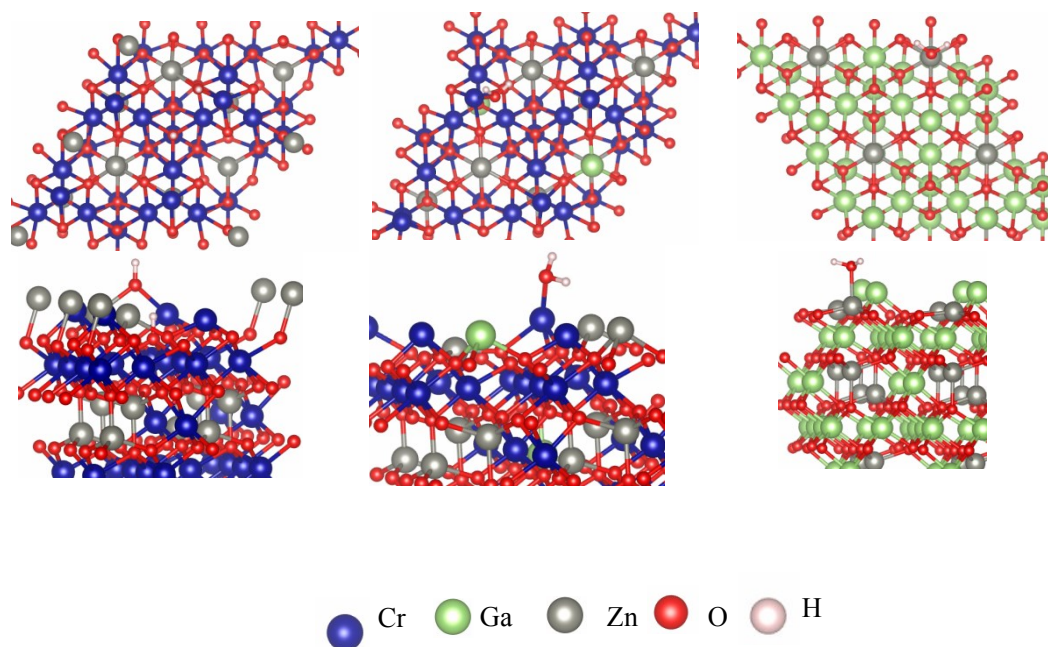
Fig. s16. The most stable adsorption configurations of H$_2$O on ZnCr$_2$O$_4$ (111) surface, ZG(111) surface, and ZnGa$_2$O$_4$ (111) surface.

surface	∠HOH	d$_{O-Me}$	d$_{O-H}$	frequency, cm^{-1} v$_{OH}$, v$_{sHOH}$
ZG (111)	107.58	2.067	0.99, 1.01	3421.59, 3037.90, 1506.56
ZnCr$_2$O$_4$ (111)		Cr-O=1.99, Zn14-O=2.07	0.97, 0.97	3756.69, 3659.04
ZnGa$_2$O$_4$ (111)	106.31	2.143	0.98，0.98	3592.07, 3485.48, 1564.54
H$_2$O	103.54		0.97, 0.98	3839.34, 3726.90, 1585.94
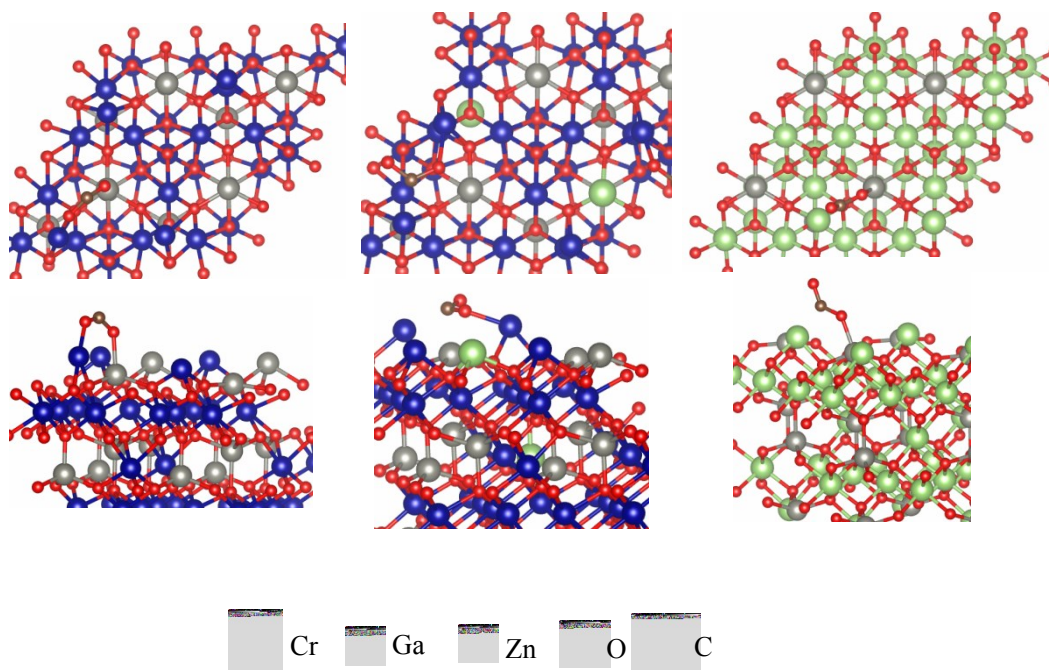
Fig. s17. The most stable adsorption configurations of CO₂ on ZnCr₂O₄ (111) surface, ZG(111) surface, and ZnGa₂O₄ (111) surface.

| surface	$\angle OCO$	$d_{O\text{-}Me}$	$d_{O\text{-}C}$	frequency, cm^{-1} $v_{sC\text{-}O}, \delta_{O\text{-}C\text{-}O}$
ZG (111)	118.95	Cr-C=2.102	1.30，1.31	1271.07，1206.28
ZnCr₂O₄ (111)	135.53	Cr-O=2.018, Zn-O=2.062	1.25, 1.25	1695.70, 1239.66, 688.63
ZnGa₂O₄ (111)	132.51	Zn-O=2.024	1.28, 1.21	1759.64, 1163.02, 713.83
CO₂	178.95		1.17, 1.19	2357.43, 1317.91, 629.92, 627.55
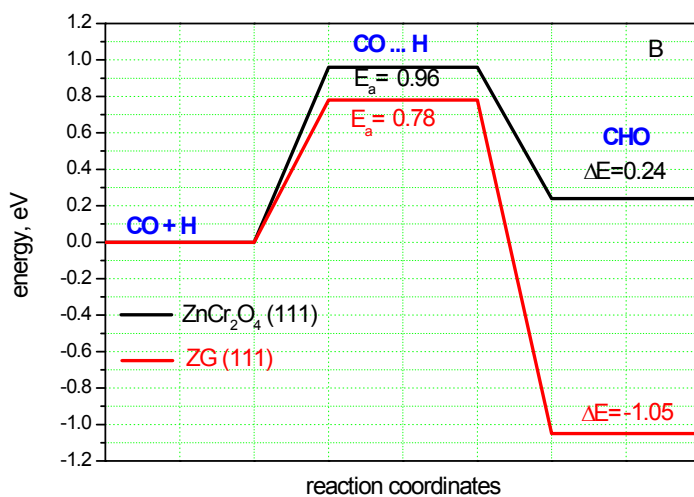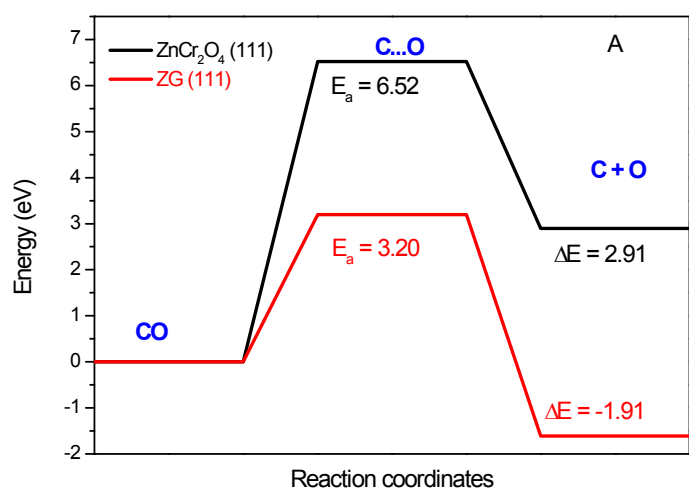
Fig. s18. Reaction coordinates of direct dissociation of CO (A) and CHO formation (B) on ZnCr₂O₄(111) and ZG(111) surfaces.
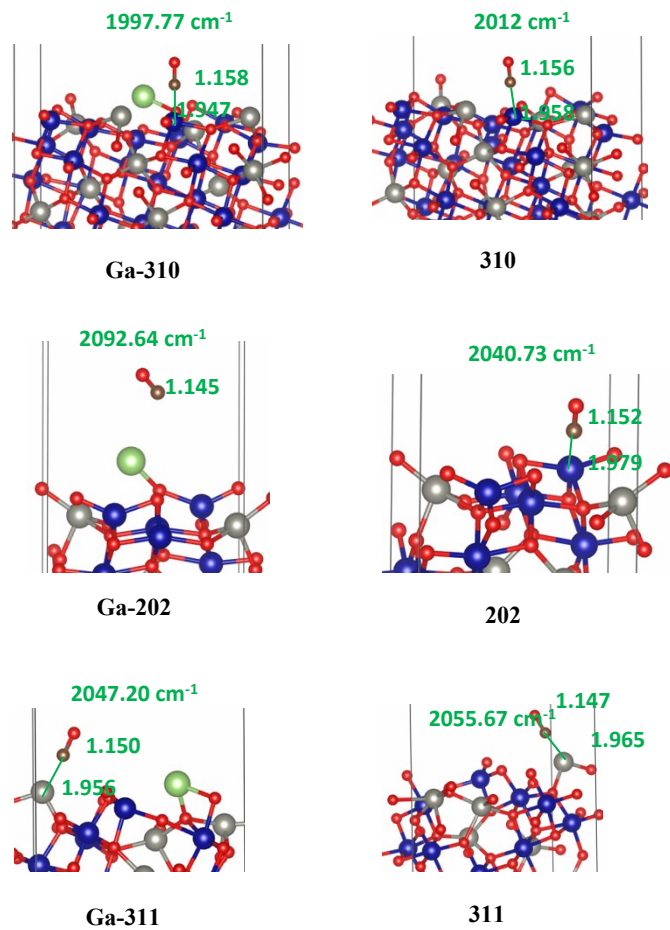
Fig.s19. The adsorption configurations and vibrational frequency of CO on (310), (202) and (311) surfaces of ZnCr₂O₄ and Ga-ZnCr₂O₄.

Table s1. The Rietveld refinement results by MAUD software for K-Ga$_x$ZnCr samples. (x=0.0, 0.55, 1.10, 1.64 and 2.18).

catalyst	ZnCr$_2$O$_4$		ZnO			sig	R$_{wp}$
	a	wt.%	a	c	wt.%		
K-Ga$_0$ZnCr	8.3629	95.2054	3.2540	5.1914	4.7946±0.0950	0.8614	12.6072
K-Ga$_{0.55}$ZnCr	8.3645	99.3184	3.2540	5.1914	0.6816±0.0761	0.8076	11.4636
K-Ga$_{1.10}$ZnCr	8.3661	95.6749	3.2481	5.2171	4.3251±0.1264	0.8823	12.2794
K-Ga$_{1.64}$ZnCr	8.3637	96.7516	3.2481	5.2171	3.2484±0.1153	0.8700	12.4247
K-Ga$_{2.18}$ZnCr	8.3590	96.4870	3.2481	5.2171	3.5130±0.1128	0.8716	12.1301
ZnO			3.2200	5.2000			
ZnCr$_2$O$_4$	8.3271						

Table s2. The total energy E_t, binding energy E_B, and reaction energy E_r for GaZnCr related reactions.

species or reactions	energy, eV		
	E_t	E_B	E_f
Zn^{2+}	-0.1645		
Cr^{3+}	-5.4867		
O^{2-}	-0.0123		
Ga^{3+}	-0.3167		
$ZnCr_2O_4$	-424.4362		
Ga_2O_3	-184.7276		
Cr_2O_3	-84.3126		
ZnO	-18.2438		
ZG	-438.5273		
CG	-334.6796		
ZGO	-19.6894		
O_2	-9.8497		
$ZnGa_2O_4$	-316.6387		
(1). $8Zn^{2+} +16Cr^{3+}+32O^{2-}=ZnCr_2O_4$		334.9394	
(2). $8Zn^{2+} +16Ga^{3+}+32O^{2-}=ZnGa_2O_4$		309.8619	
(3). $2Zn^{2+} + 2O^{2-}=ZnO$		17.8902	
(4). $4Cr^{3+} + 6O^{2-}=Cr_2O_3$		62.2920	
(5). $12Ga^{3+} + 18O^{2+} =Ga_2O_3$		180.7058	
(6). $Zn^{2+} + Ga^{3+}+2O^{2-}=ZGO$		19.1836	
(7). $7Zn^{2+} + Ga^{3+} +16Cr^{3+}+32O^{2-}=ZG$		348.8783	
(8). $8Zn^{2+} + Ga^{3+} +17Cr^{3+}+32O^{2-}=CG$		250.3528	
(9). $ZnO+Ga_2O_3=ZnGa_2O_4$			229.6797
(10). $8\ ZnO + Ga_2O_3 + 6\ ZnCr_2O_4 + 29/2\ O_2=14ZG$			192.4038
(11). $14\ ZnO + Ga_2O_3+16\ Cr_2O_3=14\ ZG+9/2\ O_2$			243.7237
(12). $16/15\ ZnO+ 1/15\ Ga_2O_3 + Cr_2O_3 = 16/15\ CG$			162.7697
(13). $ZnO+15\ ZnCr_2O_4 + Ga_2O_3=16CG$			-76.0651
(14). $2\ ZnO + Ga_2O_3 = 4\ Zn_{1/2}Ga_{1/2}O + 1/2\ O_2$			-75.0422
(15). $ZnO + Cr_2O_3 = ZnCr_2O_4$			254.7572

Tables s3. Bader charge distribution of CO and Ga on $ZnCr_2O_4$ (311), (310), (202) and (111) surfaces with and without Ga promotion.

surfaces	Bader charge
311	
Ga-311	0.4092[a]
CO/311	0.1929[b]
CO/Ga-311	-0.0112[b]/0.7650[a]
310	0
Ga-310	0.2940[a]
CO on 310	0.0182[b]
CO/Ga-310	-0.1681[b]/0.2000[a]
202	
Ga-202	0.7449[a]
CO/202	0.0482[b]
CO/Ga-202	-0.0266[b]/0.8388[a]

Note: a. bader charge on Ga; b. bader charge on CO.

Table s4. The adsorption energy of CO on the exposed $ZnCr_2O_4$ surfaces with or without Ga modification.

Surfaces	Adsorption energy of CO, eV
Ga- 202	0.03
202	-0.02
311	-0.78
Ga- 311	-0.65
Ga- 310	-0.80
310	-0.64

Table s5. XPS data for Cr2p spectras of K-Ga$_x$ZnCr samples.

catalyst	concentration, mol%					
	Cr		Cr^{3+}		Cr^{6+}	
	Area	mol,%	Area	mol,%	Area	mol,%
K-Ga$_{0.0}$ZnCr	17168.58	10.23	63456.74+65357.93	76.77	21818.66	13.00
K-Ga$_{0.55}$ZnCr	24759.53	12.27	65025.79+81071.56	72.43	30852.13	15.30
K-Ga$_{1.10}$ZnCr	13991.78	7.22	61769.33+76872.51	71.56	41084.85	21.21
K-Ga$_{1.64}$ZnCr	9970.29	5.32	91694.99+74899.72	88.97	10686.77	5.71
K-Ga$_{2.18}$ZnCr	14936.69	7.09	93622.57+84781.25	84.66	17377.78	8.25

Table s6. XPS data for Ga3d spectra of K-Ga$_x$ZnCr catalysts.

catalyst	concentration, mol%							
	Ga^{3+} at 17.06 eV		Ga^{3+} at 19.93 eV		Ga^{3+} at 21.62 eV		Ga^{3+} at 23.74eV	
	Area	mol,%	Area	mol,%	Area	mol,%	Area	mol,%
K-Ga$_{0.55}$ZnCr	1259.77	17.93	2284.44	32.52	2455.26	34.95	1025.53	14.60
K-Ga$_{1.10}$ZnCr	974.87	13.59	2309.46	32.19	2955.38	41.19	934.78	13.03
K-Ga$_{1.64}$ZnCr	1067.62	15.09	1889.29	26.70	2924.98	41.34	1193.22	16.87
K-Ga$_{2.18}$ZnCr	1406.51	18.41	1735.14	22.71	3749.57	49.08	748.80	9.80

Table s7. The surface concentration of oxygenates species of K-Ga$_x$ZnCr catalysts.

atalyst	O$_{latt}$/(O$_{latt}$ + O$_{ads}$+ O$_{OH}$)	O$_{ads}$/(O$_{latt}$ + O$_{ads}$+ O$_{OH}$)	O$_{OH}$/(O$_{latt}$ + O$_{ads}$+ O$_{OH}$)
K-Ga$_{0.0}$ZnCr	63.28	30.86	5.86
K-Ga$_{0.55}$ZnCr	60.48	34.85	4.66
K-Ga$_{1.10}$ZnCr	62.10	32.06	5.84
K-Ga$_{1.64}$ZnCr	62.51	33.38	4.11
K-Ga$_{2.18}$ZnCr	52.06	41.68	6.26

Reference

1.   D. A. Eustace, D. W. McComb and A. J. Craven, *Micron*, 2010, **41**, 547-553.

2.   G. Kresse and J. Furthmuller, *Physical Review B*, 1996, **54**, 11169-11186.

3.   G. Kresse and D. Joubert, *Physical Review B*, 1999, **59**, 1758-1775.

4.   J. P. Perdew, K. Burke and M. Ernzerhof, *Physical Review Letters*, 1996, **77**, 3865-3868.

5.   G. Henkelman, B. P. Uberuaga and H. Jonsson, *Journal of Chemical Physics*, 2000, **113**, 9901-9904.

6.   Y. Li, F. Lian, N. Chen, Z.-j. Hao and K.-c. Chou, *International Journal of Minerals, Metallurgy, and Materials*, 2015, **22**, 524-529.

7.   D. Zhou, J. Liu, S. Xu and P. Peng, *Computational Materials Science*, 2014, **86**, 24-29.

8.   D. A. Andersson and C. R. Stanek, *Phys Chem Chem Phys*, 2013, **15**, 15550-15564.

Table s8. The adsorption energy of H_2, CO, H_2O, CO_2 on ZnCr spinel and ZG surfaces.

catalyst	species and their adsorption energies			
	H_2	CO	H_2O	CO_2
$ZnCr_2O_4$ (111)	-2.88	-0.74	1.25	-1.22
ZG (111)	-1.06	-2.99	1.73	0.42
$ZnGa_2O_4$ (111)		-0.36	-1.83	-1.31